A Comparison of the Lability of Mononuclear Octahedral and Dinuclear Triple-Helical Complexes of Cobalt(II)

Loïc J. Charbonnière,[1a] Alan F. Williams,*[,1a] Urban Frey,[1b] André E. Merbach,[1b] Philippe Kamalaprija,[1c] and Olivier Schaad[1d]

Contribution from the Section of Chemistry, University of Geneva, 30 quai Ernest Ansermet, CH 1211 Geneva 4, Switzerland, and Institute of Inorganic and Analytical Chemistry, University of Lausanne, BCH, CH 1015 Lausanne, Switzerland

Received October 23, 1996[⊗]

Abstract: The lability of the mononuclear octahedral complex tris(5-methyl-2-(1′-methylbenzimidazol-2-yl)-pyridine)-cobalt(II), $[Co(\mathbf{2})_3]^{2+}$, is compared with the dinuclear triple-helical complex tris[bis[1-methyl-2-(5′-methylpyrid-2′-yl]benzimidazol-5-yl]methane]dicobalt(II), $[Co_2(\mathbf{1a})_3]^{4+}$. $[Co(\mathbf{2})_3]^{2+}$ undergoes rapid isomerization between *mer* and *fac* forms ($k_{298}(mer-fac) = 1.6 \pm 0.2\ s^{-1}$) in acetonitrile while the racemization of $(-)_{589}$-$[Co_2(\mathbf{1a})_3]^{4+}$ is roughly 10^5 times slower ($k_{298} = 1.4 \pm 2\ 10^{-5}\ s^{-1}$). The pressure dependence of the isomerization of $[Co(\mathbf{2})_3]^{2+}$ suggests a dissociatively activated process. The racemization of $(-)_{589}$-$[Co_2(\mathbf{1a})_3]^{4+}$ is found to be independent of pH above pH 4, and is not affected by added cobalt(II) or a change of solvent. Ligand exchange between $[Co_2(\mathbf{1b})_3]^{4+}$ (**1b** = bis[1-ethyl-2-(5′-methylpyrid-2′-yl)benzimidazol-5-yl]methane) and free **1a** may be followed by electrospray mass spectrocopy and establishes the mechanism of formation of the triple helix to be initial formation of mononuclear $[Co(\mathbf{1a})_3]^{2+}$ followed by capping by a second cobalt to give $[Co_2(\mathbf{1a})_3]^{4+}$. The slow racemization of $(-)_{589}$-$[Co_2(\mathbf{1a})_3]^{4+}$ is attributed to the very slow dissociation of a cobalt ion from the triple helix. This inertness is attributed to the rigidity of the ligand and the tight pitch of the helix.

Introduction

Syntheses of helical complexes (helicates) containing two or more metal ions have attracted considerable attention in recent years as examples of self-assembly reactions.[2,3] In the general strategy, multidentate ligands wrap around two or more metal ions placed along the helical axis to give double[4−7] - or triple[8−12] -helical structures, depending on the denticity of the ligating units and the coordination requirements of the metal.[13] Much attention has been paid to ligand design and to the choice of metal in order to obtain the desired structure, usually in almost quantitative yield, and the structural principles of the syntheses are now well established. Thus, if oligobidentate ligands such as **1** are used, tetrahedral metal ions will give rise to double helices, while octahedral ions will form triple helices (Figure 1).

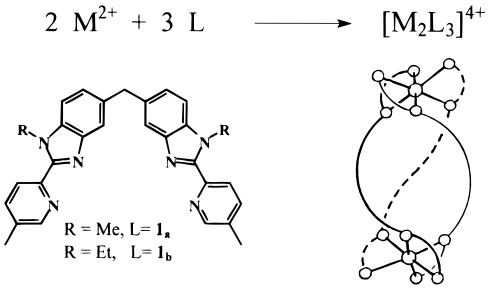

Figure 1. Strategy for the synthesis of triple-helical complexes using two octahedral metal cations.

Less attention has been paid however to the properties of these self-assembled complexes, and in particular to their chemical reactivity. In this field, only the electron transfer properties have been studied to any degree, usually by electrochemistry;[7,10,14] very little is known of the lability of the helicates. Clearly, if the complexes are to be used as starting points for further syntheses (as for example in the synthesis of a molecular knot from a dinuclear double-helical complex[15]), they must possess a degree of thermodynamic and kinetic stability. While some work has appeared on the thermodynamic stability,[13,16] the reactivity of helicates has received less attention. In the majority of cases the metal ion used for the assembly is substitutionally labile, and one might therefore reasonably expect that the resulting complexes would display the lability of their component metal ions. It was therefore surprising to discover that the enantiomerically pure triple-helical complex $(-)_{589}[Co_2(\mathbf{1a})_3]^{4+}$ (Figure 1) containing the labile Co(II) ion racemized

[⊗] Abstract published in *Advance ACS Abstracts,* February 15, 1997.

(1) (a) Department of Inorganic, Analytical and Applied Chemistry, University of Geneva; (b) Institute of Inorganic and Analytical Chemistry, University of Lausanne; (c) Department of Organic Chemistry, University of Geneva; (d) Department of Biochemistry, University of Geneva.

(2) Lindsey, J. S. *New J. Chem.* **1991**, *15*, 153.

(3) Lehn, J.-M. *Supramolecular Chemistry*; VCH Weinheim, 1995; pp 144−154.

(4) Lehn, J.-M.; Rigault, A.; Siegel, J. S.; Harrowfield, J. MacB.; Chevrier, B.; Moras, D. *Proc. Natl. Acad. Sci. U.S.A.*, **1987**, *84*, 2565.

(5) Constable, E. C.; Ward, M. D.; Tocher, D. A. *J. Chem. Soc., Dalton Trans*. **1991**, 1675.

(6) Constable, E. C. *Tetrahedron* **1992**, *48*, 10013.

(7) Potts, K. T.; Keshavarz-K, M.; Tham, F. S.; Abruña, H. D.; Arana, C. R. *Inorg. Chem.* **1993**, *32*, 4422 and following papers.

(8) Scarrow, R. C.; White, D. L.; Raymond, K. N. *J. Am. Chem. Soc.* **1985**, *107*, 6540.

(9) Libman, J.; Tor, Y.; Shanzer, A. *J. Am. Chem. Soc.* **1987**, *109*, 5880.

(10) Serr, B. R.; Andersen, K. A.; Elliott, C. M.; Andersen, O. P. *Inorg. Chem.* **1988**, *27* 4499.

(11) Williams, A. F; Piguet, C.; Bernardinelli, G. *Angew. Chem., Int. Ed. Engl.* **1991**, *30*, 1490.

(12) Krämer, R.; Lehn, J.-M.; DeCian, A.; Fischer, J. *Angew. Chem., Int. Ed. Engl.* **1993**, *32*, 703

(13) Piguet, C.; Bernardinelli, G.; Bocquet, B.; Quattropani, A.; Williams, A. F. *J. Am. Chem. Soc.* **1992**, *114*, 7440.

(14) Ferrere, S.; Elliot, C. M. *Inorg. Chem.* **1995**, *34*, 5818.

(15) Dietrich-Bucheker, C. O.; Sauvage, J.-P. *Angew. Chem., Int. Ed. Engl.* **1990**, *29*, 1154; Dietrich-Bucheker, C. O.; Sauvage, J.-P.; DeCian, A.; Fischer, J. *J. Chem. Soc., Chem. Commun.* **1994**, 2231.

(16) Pfeil, A.; Lehn, J.-M. *J. Chem. Soc., Chem. Commun.* **1992**, 838.

S0002-7863(96)03693-1 CCC: $14.00

Scheme 1. Ligand Synthesis

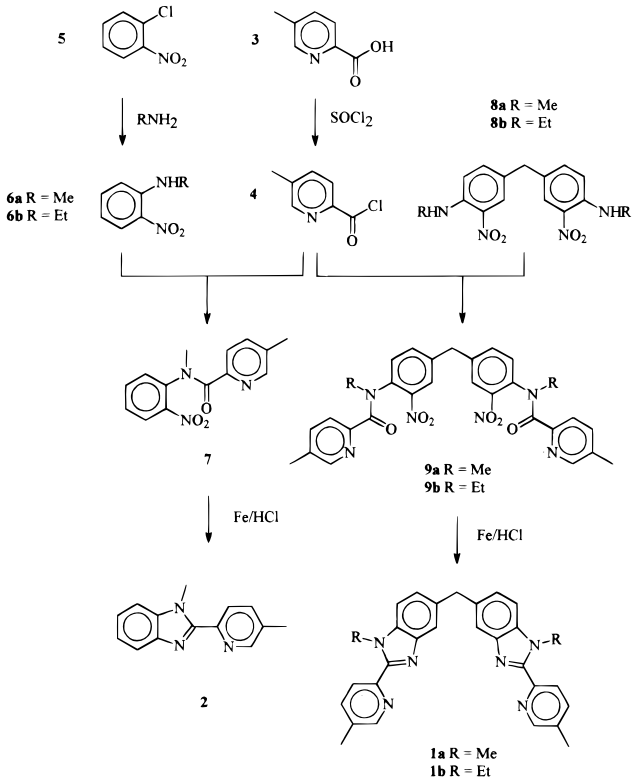

very slowly ($t_{1/2}$ = 13 h) at room temperature.[17] This suggested that self-assembled dinuclear complexes might indeed be quite inert, but two very recent studies of triple-helical systems using biscatechol ligands have shown racemization to be rapid ($t_{1/2}$ = 0.1 s) on the NMR time scale at or around room temperature.[18,19]

We have therefore sought to investigate the origin of the inertness of $[Co_2(\mathbf{1a})_3]^{4+}$. Our first step was to study the lability of the mononuclear cobalt(II) complex $[Co(\mathbf{2})_3]^{2+}$ in which the coordination sphere of the cobalt is essentially the same as that found in $[Co_2(\mathbf{1a})_3]^{4+}$; this not only establishes the inherent lability of the cobalt(II) ion in this coordination sphere but also enables a quantitative comparison with the dinuclear triple helix. Secondly, we have studied the effect on the racemization of $(-)_{589}[Co_2(\mathbf{1a})_3]^{4+}$ of pH, added cobalt(II), and solvent. Finally we have used electrospray mass spectroscopy (ESMS) to study the exchange of ligands in the triple-helical complex. The results establish clearly the formation pathway of the triple helix and give insight into the origin of the relative inertness of this complex.

Results

Synthesis. The ligands **1a**, **1b**, and **2** were synthesized using the synthetic strategy developed by Piguet[20] in which a pyridine acid chloride is reacted with an aromatic nitroamine to give a nitroamide which is then reduced and cyclized in one step with iron/hydrochloric acid to give the pyridine−benzimidazole (Scheme 1). This route is cleaner than the direct Philips coupling of a diamine and a carboxylic acid.[13]

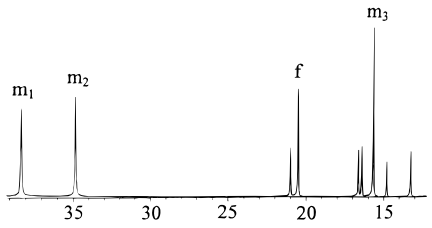

Figure 2. Part of the ^{1}H NMR spectrum of $[Co(\mathbf{2})_3]^{2+}$ showing the signals corresponding to the methyls bound to benzimidazole in the *fac* (f) and *mer* (m_1, m_2, m_3) forms.

Scheme 2. *mer*−*fac* Equilibrium of $[Co(\mathbf{2})_3]^{2+}$ [a]

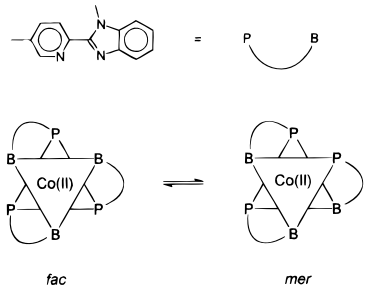

[a] *mer* and *fac* isomers are present as racemic mixtures of Δ and Λ isomers.

The complexes $[Co_2(\mathbf{1})_3]^{4+}$ and $[Co(\mathbf{2})_3]^{2+}$ were prepared by mixing stoichiometric amounts of ligand in dichloromethane or acetonitrile solution with cobalt(II) perchlorate hexahydrate in acetonitrile solution. After the solvent was stripped off under reduced pressure, the complexes could be crystallized from acetonitrile solution by slow diffusion of methanol. Enantiomerically pure $(-)_{589}[Co_2(\mathbf{1a})_3](ClO_4)_6$ was obtained by oxidation of racemic $[Co_2(\mathbf{1a})_3](ClO_4)_4$ with hydrogen peroxide and perchloric acid in acetonitrile solution in the presence of ferrocenium tetrafluoroborate as catalyst, followed by resolution of the cobalt(III) triple helix by crystallization with $(+)_{589}$-$[Sb_2(C_4H_2O_6)_2]^{2-}$.[21] Ion exhange gave the perchlorate salt. The enantiomerically pure cobalt(II) helix was generated *in situ* by reduction of $(-)_{589}$-$[Co_2(\mathbf{1a})_3](ClO_4)_6$ with sodium dithionite before kinetic runs.[17]

Behavior of the Mononuclear Complex $[Co(\mathbf{2})_3]^{2+}$. Spectroscopic titration[13] of a solution of cobalt(II) perchlorate in acetonitrile with **2** showed successive formation of $[Co(\mathbf{2})]^{2+}$, $[Co(\mathbf{2})_2]^{2+}$, and $[Co(\mathbf{2})_3]^{2+}$ with macroscopic[22] stability constants log β_1 = 7.8(1), log β_2 = 14.9(2), and log β_3 = 21.2(3). By virtue of the asymmetric nature of the ligand **2** the trisbidentate complex $[Co(\mathbf{2})_3]^{2+}$ may exist in two isomeric forms, the facial (*fac*) isomer in which the three pyridines occupy one face of the octahedron and the meridional (*mer*) complex in which they occupy a meridian of the octahedron (Scheme 2); both forms exist as pairs of Δ and Λ enantiomers. The ^{1}H NMR spectrum of a solution of $[Co(\mathbf{2})_3](ClO_4)_2$ in acetonitrile-d_3 shows a total of 36 signals spread out between +108 and −50 ppm as a result of interaction with the paramagnetic Co(II) ion. Although the rapid relaxation of the paramagnetic complex obscures proton−proton couplings, double resonance measurements allowed the differentiation of signals arising from *mer* and *fac* isomers except for eight signals arising from protons closest to the paramagnetic center which were too broad.

Integration of the signals arising from benzimidazole methyl groups of the two isomers (Figure 2) allowed the determination of the equilibrium constant K = [*fac*]/[*mer*] for the *mer*−*fac*

(17) Charbonnière, L. J.; Gilet, M.-F.; Bernauer, K.; Williams, A. F. *J. Chem. Soc., Chem. Commun.* **1996**, 39.
(18) Kersting, B.; Meyer, M.; Powers, R. E.; Raymond, K. N. *J. Am. Chem. Soc.* **1996,** *118*, 7221.
(19) Albrecht, M.; Kotila, S. *Angew. Chem., Int. Ed. Engl.* **1996**, *35*, 1208.
(20) Piguet, C.; Bocquet, B.; Hopfgartner, G. *Helv. Chim. Acta* **1994**, *77*, 931.
(21) Yoshikawa,Y.; Yamasaki, K. *Coord. Chem. Rev.* **1979**, *28*, 205.
(22) Martell, A. E.; Motekaitis, R. J. *Determination of Stability Constants* 2nd ed.; VCH: New York, 1992; Chapter 7.

isomerization as 0.23 ± 0.01 at 298 K. Studies in the temperature range 240−350 K showed a variation of this value of only a few percent and led to the thermodynamic parameters $\Delta H^\circ = +0.6 \pm 0.3$ kJ mol^{-1} and $\Delta S^\circ = -10.1 \pm 1$ J mol^{-1} K^{-1}. Note that the equilibrium constant is slightly below the statistical value of 1/3; this may arise from steric interactions between the three benzimidazoles in the *fac* isomer**.**

During the NMR experiments it was observed that irradiation of a signal of the *fac* isomer perturbed the intensity of signals of the *mer* isomer, implying chemical exchange between isomers. This suggested that NMR could be used to study the kinetics of the *mer*−*fac* exchange, and that this might be used to characterize the lability of the Co(II) center in this coordination sphere. Initial experiments used the method of Forsén and Hoffmann[23] in which the transfer of polarization between two sites is followed. However, the experiments were complicated by the short relaxation times in this paramagnetic system. The results obtained were broadly in agreement with the rates expected for a cobalt(II) system, but the precision was low. This method was therefore abandoned in favor of the NMR line broadening method in which the four proton signals (one facial, f, and three meridional, m1, m2, and m3) arising from the methyl group bound to the benzimidazole nitrogens were followed (Figure 2).

There are in principle six rate constants and three equilibrium constants needed to describe the exchange among these four different sites. However, the *mer*−*fac* isomerization requires the transformations m1 → f, m2 → f, and m3 → f to have the same rate, described by the rate constant k_{mf}. Similarly the rate constants for exchange among m1, m2, and m3 are taken to be equal and described by k_{mm}. In the slow exchange limit, the transverse relaxation rate of the ^{1}H NMR signal near the paramagnetic center, $1/T_2$, can be expressed as the sum of a term due to the paramagnetic relaxation, $1/T_{2m}$, and terms due to chemical exchanges. In this case this reduces to[24]

$$(1/T_2)^{mi} = (1/T_{2m})^{mi} + k_{mf} + k_{mm} \; (i = 1, 2, 3) \qquad (1)$$

$$(1/T_2)^{f} = (1/T_{2m})^{f} + k_{fm} \qquad (2)$$

with

$$K = [fac]/[mer] = k_{mf}/k_{fm} \qquad (3)$$

Furthermore, the temperature dependence of the pseudo-first-order exchange rate constants, k, can be expressed by eq 4 where

$$k = \frac{k_b T}{h} \exp\left(\frac{\Delta S^{\ddagger}}{R} - \frac{\Delta H^{\ddagger}}{RT}\right) = \frac{k_{298} T}{298.15} \exp\left(\frac{\Delta H^{\ddagger}}{R}\left(\frac{1}{298.15} - \frac{1}{T}\right)\right) \qquad (4)$$

$\Delta S^{\ddagger}$ and $\Delta H^{\ddagger}$ are the entropy and enthalpy of activation, respectively. An Arrhenius temperature dependence for the paramagnetic relaxation rate has been assumed (eq 5, where $(1/T_{2m})_{298}$ is the value at 298.15 K and E_m is the corresponding activation energy).

$$1/T_{2m} = (1/T_{2m})_{298} \exp[E_m/R(1/T - 1/298.15)] \qquad (5)$$

Equations 1−5 were simultaneously adjusted to the transverse relaxation rates and to the equilibrium constants (Table S1 in the Supporting Information). A plot of the temperature dependence of the relaxation rate in the form of $\ln(1/T_2)$ against $1/T$ is shown in Figure 3, and the derived kinetic, thermodynamic, and NMR parameters are given in Tables 1 and 2.

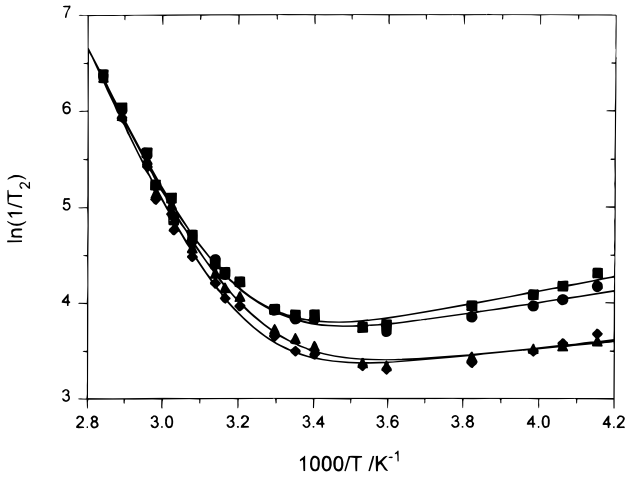

Figure 3. Temperature dependence of $1/T_2$ from the ^{1}H NMR signals of $[Co(\mathbf{2})_3]^{2+}$ in acetonitrile solution: (■) signal m1, (●) signal m2, (△) signal m3 and (◆) signal f.

To gain further information on the isomerization we have studied the effect of pressure. The pressure dependence of the rate constants was described by the linear eq 6, where the

$$\ln k = \ln k_0 - P\Delta V^{\ddagger}/RT \qquad (6)$$

volumes of activation, $\Delta V^{\ddagger}$, were assumed to be pressure independent; k_0 is the exchange rate at zero pressure. Equation 7 describes the pressure dependence of the equilibrium constant

$$\ln K = \ln K_0 - P\Delta V^{\circ}/RT \qquad (7)$$

as a function of the reaction volume ΔV° and the value at zero pressure K_0. The variable pressure measurements were made at 349.6 K, a temperature at which the paramagnetic contribution $(1/T_{2m})$ to the observed relaxation rate $(1/T_2)$ was low (<5%). Therefore, the very small pressure dependence of $1/T_{2m}$ could be neglected, and the values of $1/T_{2m}$ at zero pressure obtained from the variable temperature measurements were used. The rate and the equilibrium constants (Table S2 in the Supporting Information) were fitted to eqs 6 and 7 (Figure 4), and the results are reported in Table 1.

pH, Metal Ion, and Solvent Effects on the Racemization of $(-)_{589}[Co_2(\mathbf{1a})_3]^{4+}$. We have previously reported[17] the kinetics of racemization of the complex $(-)_{589}[Co_2(\mathbf{1a})_3]^{4+}$ as $k_{298} = (1.4 \pm 0.2) \times 10^{-5}$ s^{-1}, $\Delta H^{\ddagger} = 99 \pm 2$ kJ mol^{-1}, and $\Delta S^{\ddagger} = -6 \pm 7$ J mol^{-1} K^{-1} ($I = 0.1$ M, pH 4.75). In order to obtain further insight into the mechanism, we have investigated the influence of pH, added cobalt(II), and addition of a coordinating solvent (acetonitrile) on the kinetics of racemization.

Before studying the kinetics, the electronic spectrum of $[Co_2(\mathbf{1a})_3]^{4+}$ was studied as a function of pH in the range 1.2−11.2. The electronic spectrum was unchanged in the range pH 4−11, confirming the stability of the complex, but changed below pH 4 to yield the spectrum of the protonated ligand, the change being complete at pH 1.5. Two features are worthy of note: firstly, the change in the spectrum below pH 4 was rapid, being essentially complete within the time of mixing; secondly, the spectrum did not show any isosbestic points, and an analysis of the data in terms of only two absorbing species was not satisfactory. We conclude that, in acidic conditions, when the

(23) Forsén, S.; Hoffmann, R. A. *J. Chem. Phys.* **1963**, *39*, 2892; **1964**, *40*, 1189.

(24) Pople, J. A.; Schneider, W. G.; Bernstein, H. J. *High Resolution Nuclear Magnetic Resonance*; McGraw-Hill Book Co.: New York, 1959; p 224.

Table 1. Derived Kinetic and Thermodynamic Parameters for the Variable Temperature and Pressure Studies

	mer−*fac* isomerization	*mer* interconversion		*mer*−*fac* isomerization	*mer* interconversion
k_{298}/s^{-1}	1.6 ± 0.2	7.6 ± 0.7	$\Delta S^{\ddagger}/(J\ mol^{-1}K^{-1})$	−10.8 ± 8	−20.1 ± 6
$\Delta H^{\ddagger}/(kJ\ mol^{-1})$	68.7 ± 3	62.0 ± 2	$\Delta V^{\ddagger}/(cm^3\ mol^{-1})^a$	+6.3 ± 0.4	+5.4 ± 0.2

	mer−*fac* isomerization		*mer*−*fac* isomerization
K_{298}	0.23 ± 0.01	$\Delta S°/(J\ mol^{-1}\ K^{-1})$	−10.1 ± 1
$\Delta H°/(kJ\ mol^{-1})$	0.6 ± 0.3	$\Delta V°/(cm^3\ mol^{-1})^a$	+0.8 ± 0.3

[a] At 349.6 K: $(k_{mf})_0 = 107 \pm 2\ s^{-1}$, $(k_{mm})_0 = 327 \pm 3\ s^{-1}$, $K_0 = 0.25 \pm 0.01$.

Table 2. Derived NMR Parameters for the Variable Temperature Study

	m1	m2	m3	f
$(1/T_{2m})_{298}/s^{-1}$	37 ± 1	36 ± 1	26 ± 1	26 ± 1
$E_m/(kJ\ mol^{-1})$	6.4 ± 0.6	5.2 ± 0.6	3.3 ± 0.6	3.7 ± 0.7

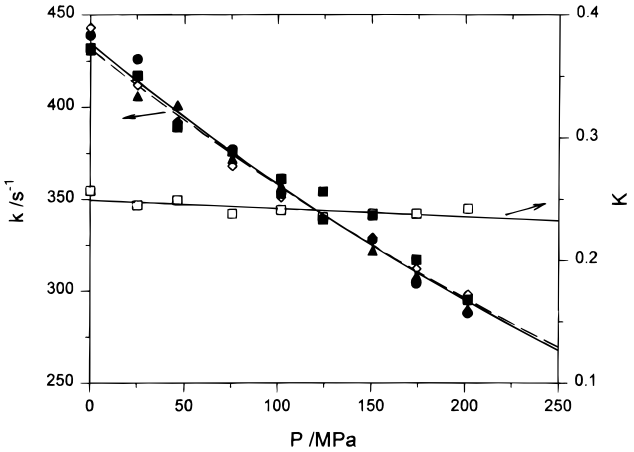

Figure 4. Pressure dependence of the rate constants $k_{mm} + k_{mf}$ (solid line, (■) signal m1, (●) signal m2, and (△) signal m3) and k_{fm} (dashed line, (◇ signal f) and pressure dependence of the equilibrium constant K (□) for the intramolecular exchanges of $[Co(\mathbf{2})_3]^{2+}$ in acetonitrile solution.

triple helix is thermodynamically unstable, the cobalt(II) ion shows its expected lability, and that the decomplexation takes place *via* an intermediate.

Further kinetic experiments were carried out at 323 K, where the half-life for racemization is on the order of 30 min. Measurements at pH 5.07, 4.75, 4.26, and 4.02 (acetate buffer, $I = 0.1$M) gave rate constants of (3.8 ± 0.3), (3.7 ± 0.4), (3.2 ± 0.3), and (4.6 ± 0.4) × 10^{-4} s^{-1} for racemization. Only the last value, measured at pH 4.02, shows any significant change, and we assume that this is due to the onset of the dissociation of the complex in acid; above pH 4, however, the racemization rate is independent of pH. If the mechanism of racemization requires a rapid preequilibrium dissociation of one of the cobalt(II) ions, then the addition of free Co^{2+} would be expected to slow the rate. Measurements with 0, 1.3, and 100 equiv of cobalt(II) perchlorate hexahydrate added to the solution gave rate constants of (4.0 ± 0.4), (2.9 ± 0.5), and (4.2 ± 0.2) × 10^{-4} s^{-1}, respectively, showing no retardation effect. Finally, the racemization was studied in aqueous solution diluted with an equal volume of acetonitrile, giving a rate constant of (2.8 ± 0.4) × 10^{-4} s^{-1}, slightly lower than that for the purely aqueous solution (4.0 × 10^{-4} s^{-1}). The rate is thus not very sensitive to the presence of coordinating solvent contrary to our observations with a copper(I) double helix.[25]

Ligand Exchange in $[Co_2(\mathbf{1})_3]^{4+}$ Followed by Electrospray Mass Spectrometry. It has been established previously[13] that replacement of the methyl substituents of the benzimidazoles by ethyls in ligands related to **1a** does not affect formation of the triple helix, and the ^{1}H NMR spectrum of $[Co_2(\mathbf{1b})_3]^{4+}$ confirms that a triple-helical complex is formed. The exchange of ligand **1b** for **1a** offers therefore a means of studying the exchange of two practically identical ligands in a $[Co_2(\mathbf{1})_3]^{4+}$ complex. Attemps to follow the exchange by ^{1}H NMR spectroscopy were unsuccessful because of the complexity of the spectra. We therefore turned to electrospray mass spectrometry (ESMS) which distinguishes between ligands **1a** and **1b** by their different molecular masses.

For ESMS to be applicable to this problem, one must be able to identify unambiguously the different peaks observed in the spectrum and to relate their intensities to the relative concentration of the complexes. We have previously reported[26] that the triple-helical complexes of cobalt(II) give clean mass spectra in solution under ESMS conditions, the only significant peaks being the molecular ions M^{n+} (the base peak) and $M(X)^{(n-1)+}$ where X^- is the monovalent counter anion with an intensity typically 10% that of the base peak. In agreement with this, the ESMS spectrum of $[Co_2(\mathbf{1a})_3]^{4+}$ has the base peak at m/z = 373.1 and that of $[Co_2(\mathbf{1b})_3]^{4+}$ at m/z = 394.2. Neither compound shows significant fragmentation in the conditions used. We may therefore attribute peaks between m/z = 373 m/z = and 394 to the formation of mixed ligand species.

The correlation of peak intensities to relative abundance in solution is in general less straightforward. For the compounds studied here, however, it is quite reasonable, since we are comparing species of the same charge, with the same basic structure, and very similar size (the difference in mass between the heaviest and lightest ion is just over 5%), and none undergo fragmentation. Results in the literature[27,28] show good agreement between speciations obtained by ESMS and those obtained from NMR and spectroscopic titration for this type of compound. To confirm the validity of this assumption, we have carried out a scrambling experiment.

A volume of $[Co_2(\mathbf{1a})_3](ClO_4)_4$ (4.1×10^{-5} M in acetonitrile) was added to an equal volume of $[Co_2(\mathbf{1b})_3](CF_3SO_3)_4$ (3.1×10^{-5} M in acetonitrile), and the ESMS spectrum was recorded at regular intervals. Figure 5 shows the evolution of the $[Co_2(\mathbf{1a})_{3-x}(\mathbf{1b})_x]^{4+}$ region of the spectrum with time. It will be seen that the mixed ligand species $[Co_2(\mathbf{1a})_2(\mathbf{1b})]^{4+}$ and $[Co_2(\mathbf{1a})(\mathbf{1b})_2]^{4+}$ grow in slowly and no other signals are seen. The ratio of the observed peak intensities after 3 h corresponds to the statistical ratio expected if the intensities are proportional to concentration. Throughout the experiment the only peaks

(25) Rüttimann, S.; Piguet, C.; Bernardinelli, G; Bocquet, B.; Williams, A. F. *J. Am. Chem. Soc.* **1992,** *114*, 4230.

(26) Hopfgartner, G.; Piguet, C.; Henion, J. D.; Williams, A. F. *Helv. Chim. Acta* **1993**, *76*, 1759. Hopfgartner, G.; Piguet, C.; Henion, J. D. *J. Am. Soc. Mass Spectrom.* **1994**, 5, 748.

(27) Piguet, C.; Hopfgartner, G.; Bocquet, B.; Schaad, O.; Williams, A. F. *J. Am. Chem. Soc.* **1994**, *116*, 9092.

(28) Marquis-Rigault, A.; Dupont-Gervais, A.; Van Dorsselaer, A., Lehn. J.-M. *Chem. Eur. J.* **1996**, *2*, 1395.

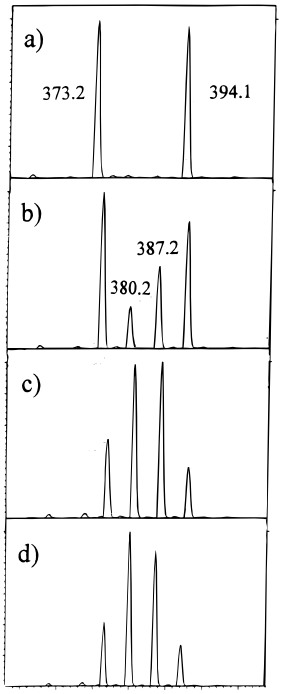

Figure 5. Base peak of the ESMS spectrum of a mixture of equal volumes of $[Co_2(\mathbf{1a})_3](ClO_4)_4$ (4.1×10^{-5} M) and $[Co_2(\mathbf{1b})_3](CF_3SO_3)_4$ (3.1×10^{-5} M) in acetonitrile after (a) 5, (b) 67, (c) 190, and (d) 368 min.

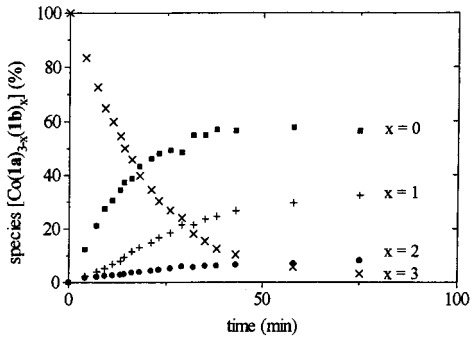

Figure 6. Intensities of the peaks due to $[Co_2(\mathbf{1a})_x(\mathbf{1b})_{3-x}]^{4+}$ ($x = 0-3$) as a function of time in the ESMS spectrum: (×) $[Co_2(\mathbf{1b})_3]^{4+}$, (●) $[Co_2(\mathbf{1a})(\mathbf{1b})_2]^{4+}$, (+) $[Co_2(\mathbf{1a})_2(\mathbf{1b})]^{4+}$, (■) $[Co_2(\mathbf{1a})_3]^{4+}$.

of importance were $[Co_2(\mathbf{1a})_{3-x}(\mathbf{1b})_x]^{4+}$ or the adduct with one counter anion.

With the significance of the peak intensities established, it is now possible to follow the exchange of free ligand with the complex. In a second experiment, equal volumes of a solution of $[Co_2(\mathbf{1b})_3](CF_3SO_3)_4$ (3.1×10^{-5} M in acetonitrile) and a solution of **1a** (2.3×10^{-4} M in acetonitrile, i.e., 7.4 mol of **1a**/mol of $[Co_2(\mathbf{1b})_3](CF_3SO_3)_4$) were mixed together, and the ESMS spectra recorded as a function of time. Figure 6 shows the variation of the intensity of the peaks corresponding to $[Co_2(\mathbf{1a})_x(\mathbf{1b})_{3-x}]^{4+}$ ($x = 0-3$) as a function of time. As expected, in view of the great excess of **1a**, the signal due to $[Co_2(\mathbf{1b})_3]^{4+}$ falls away rapidly, but the surprising observation is that it is $[Co_2(\mathbf{1a})_3]^{4+}$ which grows fastest, the mixed species $[Co_2(\mathbf{1a})_x(\mathbf{1b})_{3-x}]^{4+}$ ($x = 1$ or 2) only appearing later and more slowly. Throughout the experiment, the spectrum is dominated by the peaks due to $[Co_2(\mathbf{1a})_x(\mathbf{1b})_{3-x}]^{4+}$ ($x = 0-3$), but weak peaks are now observed for species $[Co_2(\mathbf{1a})_x(\mathbf{1b})_{4-x}]^{4+}$ ($x = 0-4$) and $[Co(\mathbf{1a})_x(\mathbf{1b})_{3-x}]^{2+}$ ($x = 0-3$). The presence of these species, typically a few percent of the base peak, is a result of the considerable excess of ligand present in solution during this experiment.

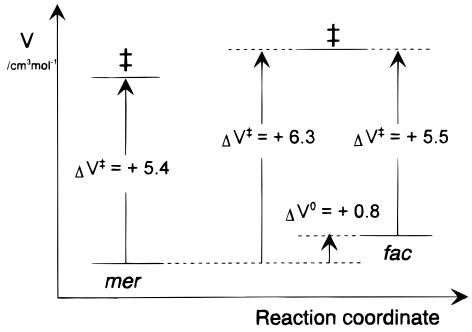

Figure 7. Volume profile for the intramolecular exchanges.

Scheme 3. Formation Routes for $[M_2L_3]$

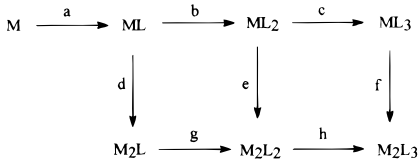

Discussion

The value for the equilibrium constant (Table 1) for the *mer*−*fac* isomerization of $[Co(\mathbf{2})_3]^{2+}$ is slightly lower than the statistical value of 1/3. We attribute this to a greater steric repulsion when the three benzimidazole moieties are constrained to lie on the same face of the octahedron, and this is supported by the positive values of ΔH° and ΔV° for the reaction (Figure 7). The kinetics of the isomerization show the expected lability of a high-spin cobalt(II) center, and the rate constants for the exchange processes are comparable with the value of 6.9 s^{-1} reported[29] for the racemization of $[Co(phen)_3]^{2+}$ in water. The activation parameters for the *mer*−*mer* and *mer*−*fac* processes are sufficiently close to suggest that they pass through a similar transition state, which, given the positive $\Delta V^\ddagger$ values, is dissociatively activated, as observed for solvent exchange at cobalt(II) centers.[30] Although the small negative value of the entropy of activation is in contradiction with a dissociative mode of activation, the difficulties encountered in using $\Delta S^\ddagger$ to assign a reaction pathway have been discussed elsewhere.[31] The factors which affect this parameter are poorly understood, and nonrandom errors are often associated with the determination of $\Delta S^\ddagger$. The kinetic data for $[Co(\mathbf{2})_3]^{2+}$ clearly establish that the coordination sphere of three benzimidazole−pyridine units does not possess an inherent inertness which might explain the slow racemization of $[Co_2(\mathbf{1a})_3]^{4+}$. At 298 K the ratio of the rate constant for racemization of triple-helical $[Co_2(\mathbf{1a})_3]^{4+}$ to that for exchange between two sites in the *mer* isomer of $[Co(\mathbf{2})_3]^{2+}$ is 1.8×10^{-6}. Examination of the activation parameters for the two processes shows that this difference arises essentially from the considerable increase in the activation enthalpy from 69(3) kJ mol^{-1} for $[Co(\mathbf{2})_3]^{2+}$ to 99(2) kJ mol^{-1} for $[Co_2(\mathbf{1a})_3]^{4+}$.

Before addressing the question of the inertness of $[Co_2(\mathbf{1a})_3]^{4+}$, we note that the ESMS data allow us to clarify the pathways for complex formation and dissociation in the triple-helical system. We have previously noted that formation of the triple-helical complex, as followed by spectroscopic titration, is rapid.[32] The possible routes to a triple-helical complex M_2L_3 are shown in Scheme 3. The final step of formation may occur in two ways: (i) route f, in which a preformed *fac*-ML_3 complex

(29) Blinn, E. L.; Wilkins, R. G. *Inorg. Chem.* **1976**, *15*, 2952.
(30) Lincoln, S. F; Merbach, A. E. *Adv. Inorg. Chem.* **1995**, *42*, 1
(31) Newman, K. E.; Meyer, F. K.; Merbach, A. E. *J. Am. Chem. Soc.* **1979**, *101*, 1470
(32) Piguet, C.; Bernardinelli, G.; Bocquet, B.; Schaad, O.; Williams, A. F. *Inorg. Chem.* **1993**, *33*, 4112.

binds a second metal to give M_2L_3 (we will call this the keystone mechanism), and (ii) route h, in which a third ligand is added to a preformed M_2L_2 complex (we will call this the braiding mechanism). The braiding mechanism might at first sight appear attractive since we have shown[13] that a rapid equilibrium exists between M_2L_2 and M_2L_3 for M = Zn(II).

If we assume microscopic reversibility, then the dissociation of the M_2L_3 complex will occur either by eq 8 according to the

$$M_2L_3 \rightarrow ML_3 + M \quad (8)$$

keystone mechanism or by eq 9 according to the braiding mechanism. The ESMS results for $[Co_2(\mathbf{1b})_3]^{4+}$ in the presence

$$M_2L_3 \rightarrow M_2L_2 + L \quad (9)$$

of excess **1a** allow us to eliminate the braiding mechanism, since in the presence of an excess of a second ligand L′ (in practice **1a**), the M_2L_2 intermediate will react with L′ to form the mixed ligand species M_2L_2L'. We would therefore expect the rapid apparition of mixed ligand species, with M_2L_2L' appearing before $M_2L'_3$, contrary to experiment. The keystone mechanism does however explain this result. After dissociation of M according to eq 8, the free metal ion will be complexed by the excess free ligand, which is exclusively L′ at the beginning of the experiment:

$$M + 3L' \rightarrow ML'_3 \quad (10)$$

As more M is released into the solution (by reaction 8 and the reverse of reaction 10), the ML'_3 will capture it to give $M_2L'_3$; it is only as the experiment proceeds, and the amount of free L in solution increases to where it is comparable with free L′, that mixed ligand species will be formed. This is exactly what is observed in Figure 6. Thus, the ESMS data establish the formation route of $[Co_2(\mathbf{1})_3]^{4+}$ to be a−b−c−f as shown in Scheme 3. The first step is formation of mononuclear $[Co(\mathbf{1})_3]^{2+}$ which is then locked into an inert structure by complexation of a second metal ion in the same way that the keystone of an arch confers stability on the structure as a whole. The weak peaks in the ESMS spectrum due to $[Co_2(\mathbf{1a})_x(\mathbf{1b})_{4-x}]^{4+}$ ($x = 0-4$) and $[Co(\mathbf{1a})_x(\mathbf{1b})_{3-x}]^{2+}$ ($x = 0-3$) are also consistent with this mechanism, the first species arising from interaction of free ligand with *mer*-$[Co_2(\mathbf{1a})_x(\mathbf{1b})_{3-x}]^{4+}$ ($x = 0-3$) in which one cobalt is octahedrally coordinated and the second is bound to only two benzimidazole−pyridines, and is thus coordinatively unsaturated. There is some precedent for this in the literature: a study of the formation of trinuclear double helicates by spectroscopic titration showed the successive formation of ML_2, M_2L_2, and M_3L_2.[16]

The slow racemization of the triple helix may be understood in terms of a dissociative mechanism (eq 11). The rate-

$$\Delta\text{-}M_2L_3 \xrightarrow{\text{slow}} \Delta\text{-}\textit{fac}\text{-}ML_3 + M \underset{}{\overset{\text{fast}}{\rightleftharpoons}} \Lambda\text{-}\textit{fac}\text{-}ML_3 + M \xrightarrow{\text{fast}} \Lambda\text{-}M_2L_3 \quad (11)$$

$$\text{rac-}\textit{mer}\text{-}ML_3$$

determining step is thus the loss of M from the triple-helical complex (eq 8), which is expected to show first-order kinetics. This possibility was not considered in our previous communication.[17] Although the individual cobalt−nitrogen bonds are labile, the rigid structure of the helix will maintain the dissociated nitrogen atom very close to the metal ion, and consequently a greater degree of bond breaking is necessary to allow the dissociation of cobalt from a pyridine−benzimidazole unit than for the mononuclear species. This explains the increase in $\Delta H^{\ddagger}$. It is only when the pH is sufficiently low (<4) for the proton to compete with the cobalt for nitrogen donors that the recombination reaction is prevented, and the complex dissociates rapidly.

Chart 1

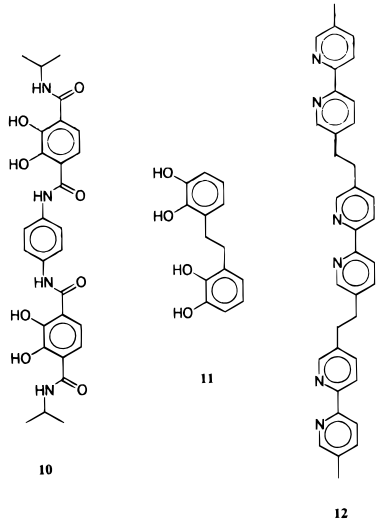

The Bailar twist offers an alternative mechanism for racemization of a trisbidentate complex and has recently been observed for another triple-helical complex.[18] The triple-helical complex $[Ga_2(\mathbf{10})_3]^{6-}$ (Chart 1) studied by Raymond and co-workers was shown to undergo inversion via a Bailar twist mechanism passing through the Δ,Λ-complex (or *meso*-helicate) as an intermediate with $\Delta G^{\ddagger}_{298} = 79 \pm 2$ kJ mol^{-1}, against $\Delta G^{\ddagger}_{298} = 101 \pm 4$ kJ mol^{-1} for $[Co_2(\mathbf{1a})_3]^{4+}$. In this case the $\Delta G^{\ddagger}_{298}$ was only 12 kJ mol^{-1} higher than that of the equivalent mononuclear complex,[33] in sharp contrast to the difference between $[Co_2(\mathbf{1a})_3]^{4+}$ and $[Co(\mathbf{2})_3]^{2+}$. Albrecht and Kotila[19] have reported the value of $\Delta G^{\ddagger}_{233} = 43$ kJ mol^{-1} for the triple helix $[Ti_2(\mathbf{11})_3]^{4-}$; since the structure reported for this compound shows the titanium coordination to be quite close to trigonal prismatic, the transition state geometry for the Bailar twist, it seems most probable that this complex also racemizes by a Bailar twist. We may confidently exclude a Bailar twist mechanism for $[Co_2(\mathbf{1a})_3]^{4+}$. The trigonal prismatic transition state requires the two coordinating atoms of the chelate ring to lie approximately parallel to the C_3 symmetry axis of the triple helix. It is not possible for ligand **1a** to achieve this at one metal site while coordination of the cobalt is maintained at the other. By virtue of the repulsions between the hydrogen atoms in position 4 of the benzimidazole units, ligand **1** cannot be planar, and the distribution of the four coordinating atoms in space forms a spiral: this spiral can be right handed or left handed, but the chirality cannot be changed while the integrity of the $[Co_2(\mathbf{1a})_3]^{4+}$ complex is maintained.

The constraints due to the ligand may also be seen in the solid state stuctures, most particularly in the pitch of the helix. If $\mathbf{a}_n$ and $\mathbf{b}_n$ are the coordinates of the two atoms of the chelate unit bound to metal $\mathbf{M}_n$, then we may define a midpoint of the chelate $\mathbf{x}_n$ as $(\mathbf{a}_n + \mathbf{b}_n)/2$, and estimate the twisting of the helix by the torsion angle $\mathbf{x}_1-\mathbf{M}_1-\mathbf{M}_2-\mathbf{x}_2$, divided by the metal−metal distance $|\mathbf{M}_1-\mathbf{M}_2|$. The pitch, defined as the displacement along the axis required for a complete turn, is given by $360/\theta$ Å. For $[Ga_2(\mathbf{10})_3]^{6-}$ the pitch calculated in this way is 58.3 Å compared to 19.9 Å for $[Co_2(\mathbf{1a})_3]^{4+}$, differing by a factor of 3, while for the even more rapidly inverting $[Ti_2(\mathbf{11})_3]^{4-}$ the

(33) Kersting, B.; Telford, J. R.; Meyer, M.; Raymond, K. N. *J. Am. Chem. Soc.* **1996**, *118*, 5712.

pitch is still greater (ca. 220 Å).[19] The shorter the pitch, the harder it will be to untwist the helix to pass through the trigonal prismatic transition state required by the Bailar mechanism. This leads to the interesting hypothesis that introducing a certain curvature into the disposition of the ligating atoms will shorten the pitch and slow the racemization.

The only other triple helix for which racemization data are available is the trinuclear triple helix $[Ni_3(\mathbf{12})_3]^{6+}$ which was reported by Lehn *et al.* to racemize with a rate constant of 1.5×10^{-6} s^{-1} at room temperature.[12] The trinuclear species is indeed slower than the mononuclear species $[Ni(bipy)_3]^{2+}$,[34] but the factor is only on the order of 500, 3 orders of magnitude less than observed for $[Co_2(\mathbf{1a})_3]^{4+}$. The racemization of $[Ni(phen)_3]^{2+}$ has been assigned a dissociative pathway,[35] and assuming this also to be true for $[Ni_3(\mathbf{12})_3]^{6+}$ we might anticipate a deceleration similar to that observed in our results. We attribute the small magnitude of the effect to the greater degree of flexibility in **12** than in **1**, and to the much greater pitch of $[Ni_3(\mathbf{12})_3]^{6+}$, 48.2 Å, more than twice that of $[Co_2(\mathbf{1a})_3]^{4+}$. The lesser twisting, and the greater degree of flexibility, will facilitate the loss of a nickel from one site without disruption of the other, and will also lower the energetic barrier to a Δ,Λ-complex as an intermediate. It will be noted that the two metal ions with partially filled d-shells, Co(II) and Ni(II), are both much slower to racemize than the ions Ga(III) (d^{10}) and Ti(IV) (d^0) studied by Raymond[18] and Albrecht.[19]

In conclusion, we have shown that the coordination sphere of the mononuclear complex $[Co(\mathbf{2})_3]^{2+}$ shows the lability expected for a cobalt(II) center. The inertness of $[Co_2(\mathbf{1a})_3]^{4+}$ is thus a supramolecular effect, arising from the rigidity of the structure as a whole. We have shown how electrospray mass spectroscopy may be used to follow ligand exchange reactions by the use of ligands with different peripheral substituents. The results show the complex to be formed by initial assembly of three ligands around one metal followed by the complexation of the second to the preorganized hexadentate site. Each metal thus holds in place the coordination site for the other, leading to remarkable kinetic stability for the cobalt(II) ion. Comparison with other triple-helical systems suggests that $[Co_2(\mathbf{1a})_3]^{4+}$ owes its remarkable inertness to the rigidity of the ligand **1** which results in a very tight pitch. Careful design of the spacing group may therefore be used to control the lability of the helical complex.

Experimental Section

Materials. Solvents and starting materials were purchased from Fluka AG (Buchs, Switzerland) and used without further purification unless otherwise stated. Aluminum oxide (Merck activity I or II−III, 0.063−0.200 mm) and silica gel (Merck, 0.063−0.200 mm) were used for preparative column chromatography. 2-Carboxy-5-methylpyridine (**3**),[32] bis[3-nitro-4-(*N*-methylamino)phenyl]methane (**8a**),[13] bis[3-nitro-4-bis(*N*-ethylamino)phenyl]methane (**8b**),[13] and the complex $[Co_2(\mathbf{1a})_3](ClO_4)_4$[32] were prepared according to literature procedures.

Ligand Synthesis. Preparation of Bis[3-nitro-4-[methyl[(5-methylpyridin-2-yl)carbonyl]amino]phenyl]methane (9a). A 300 mg (2.18 mmol) sample of acid **3** was dissolved in 45 mL of dry CH_2Cl_2 (filtered on Alox Act. I), and 1.6 mL (21.7 mmol) of $SOCl_2$ was added with a few drops of DMF. A white precipitate formed which slowly disappeared on refluxing the solution for 1 h, with a $CaCl_2$ tube capping the reflux condenser. The solution was evaporated to dryness and the oily residue dried under vacuum for 30 min. The solid was dissolved in 25 mL of dry CH_2Cl_2 containing 280 mg (0.79 mmol) of diamine **8a** and 1.14 mL of Et_3N, and the solution was heated to reflux for 18 h. After cooling, the solution was extracted with 50 mL of water and 50 mL of 10% $(NH_4)_2SO_4$ in water. The aqueous fractions were washed with 20 mL of CH_2Cl_2 and the organic layers gathered, filtered over cellulose, and evaporated to dryness. The resulting solid was purified by column chromatography over silica (50 g, CH_2Cl_2/MeOH, 99/1) to give **9a** as a pale brown solid which decomposes above 62 °C. Yield: 378 mg (86%). $R_f = 0.54$ on Alox TLC (CH_2Cl_2/MeOH, 99/1). Anal. Calcd for $C_{29}H_{26}N_6O_6$: C, 62.80; H, 4.73; N, 15.16. Found: C, 62.69; H, 5.00; N, 14.89. EI/MS: $m/z = 508$ (M − NO_2), 462 (M − $2NO_2$).

Preparation of Bis[3-nitro-4-[ethyl[(5-methylpyridin-2-yl)carbonyl]amino] phenyl]methane (9b). 9b was obtained by the same procedure as for **9a**, starting from 500 mg of the acid **3** and 2.7 mL of $SOCl_2$ in 65 mL of dry CH_2Cl_2. In the second step, the solid was dissolved in 30 mL of CH_2Cl_2 containing 420 mg (1.22 mmol) of the diamine **8b** and 2.6 mL of Et_3N. After workup and chromatography on silica (CH_2Cl_2/MeOH, 99/1) **9b** was obtained as a pale brown solid which decomposes above 62 °C. Yield: 650 mg (92%). $R_f = 0.36$ on Alox TLC (CH_2Cl_2/MeOH, 99/1). EI-MS: $m/z = 583$ (M + H^+), 536 (M − NO_2). ^{1}H-NMR in $CDCl_3$: δ 1.12, 1.27 (2t, 6H, $^3J = 7$ Hz); 2.20, 2.40 (2s, 6H, br); 3.71, 4.22 (m, 4H, br); 4.06 (s, 2H, br); 7.30−8.50 (m, 12H, br). The spectrum shows the presence of more than one conformation as a result of restricted rotation of the amide[20] and results in broad poorly resolved signals.

Preparation of Bis[1-methyl-2-(5-methylpyrid-2-yl)benzimidazol-5-yl] methane (1a). A 369 mg sample of the diamide **9a** (0.67 mmol) was dissolved in 100 mL of absolute ethanol with 20 mL of distilled water, 3.9 mL of concentrated HCl (47 mmol), and 1.12 g of activated iron (20.1 mmol). The solution was refluxed under nitrogen for 14 h. The iron was filtered and ethanol evaporated under reduced pressure. A 20 mL sample of water containing 10 g of Na_2H_2EDTA (26.9 mmol) was added to the solution and the mixture stirred vigorously with 100 mL of CH_2Cl_2 while the pH was increased to 9 with concentrated NH_4OH. The aqueous layer was then further extracted with three portions of 100 mL of CH_2Cl_2. The combined organic layers were dried over Na_2SO_4, filtered over cellulose, evaporated to dryness, and purified by column chromatography over silica (30 g, CH_2Cl_2/MeOH, 95/5). **1a** is obtained as a white solid. Yield: 265 mg (87%). The analysis and spectra correspond to the results of the literature.[32]

Preparation of Bis[1-ethyl-2-(5-methylpyrid-2-yl)benzimidazol-5-yl] methane (1b). 1b was obtained analogously to **1a** starting from diamide **9b** in 87% yield after purification. Anal. Calcd for $C_{31}H_{30}N_6$: C, 76.50; H, 6.23; N, 17.27. Found: C, 76.24; H, 6.25; N, 17.36. EI/MS: $m/z = 486$ (M^+); 471 (M − CH_3); 457 (M − C_2H_5). ^{1}H-NMR in $CDCl_3$: δ 1.44 (t, 6H, $^3J = 7$ Hz), 2.40 (s, 6H), 4.26 (s, 2H), 4.81 (q, 4H, $^3J = 7.2$ Hz), 7.19 (dd, 2H), 7.23 (dd, 2H), 7.62 (m, 2H), 7.68 (m, 2H), 8.27 (dd, 2H), 8.51 (m, 2H). ^{13}C-NMR in $CDCl_3$: δ 15.3, 18.4 (primary C); 40.4, 42.2 (secondary C); 109.7, 119.7, 124.0, 124.4, 137.2, 149.0 (tertiary C); 133.3, 134.7, 136.2, 142.9, 148.1, 149.9 (quaternary C).

Preparation of 5-Methylpyridine-2-carboxylic Acid *N*-Methyl-*N*-(2-nitrophenyl)amide (7). A 1 g sample of acid **3** (7.3 mmol) was dissolved in 100 mL of dry CH_2Cl_2 with a few drops of DMF and 5.3 mL of $SOCl_2$ (73 mmol) added dropwise over 10 min. A white precipitate formed which slowly disappeared while the solution was refluxed for 1 h with a $CaCl_2$ tube capping the reflux condenser. The solution was then evaporated to dryness and the solid coevaporated twice with 30 mL of CH_2Cl_2 and finally dried under vacuum (10^{-2} Torr, 30 min). The solid was dissolved in 60 mL of dry CH_2Cl_2 and a solution containing 1.22 g of **6a** (7.3 mmol) and 5.2 mL of Et_3N (73 mmol) in 60 mL of dry CH_2Cl_2 added dropwise for 15 min under constant stirring. The deep green solution was refluxed for 5 h under nitrogen and evaporated to dryness. The solid was dissolved in 250 mL of CH_2Cl_2 and washed with 250 mL of 10% $(NH_4)_2SO_4$ in water. The aqueous layer was washed twice with 150 mL of CH_2Cl_2. The combined organic layers were dried over Na_2SO_4, filtered, and evaporated to dryness. The oily residue was purified by column chromatography over alumina (CH_2Cl_2/MeOH, 99.5/0.5). After drying, **7** was obtained as a pale brown solid which decomposes above 127 °C. Yield: 1.43 g (72%). ^{1}H-NMR in $CDCl_3$: δ 2.39 (s, 3H, br); 3.47 (s, 3H, br); 7.29−8.43 (m, 7H, br). EI-MS: $m/z = 225$ (M-NO_2). $R_f = 0.26$ (silica TLC, CH_2Cl_2/MeOH, 98/2).

Preparation of 5-Methyl-2-(1-methylbenzimidazol-2-yl)pyridine (2). A 604 mg sample of **7** (2.2 mmol) was dissolved in 100 mL of absolute ethanol containing 30 mL of distilled water, 6.4 mL of

(34) Schweitzer, G. K; Lee, J. M *J. Phys. Chem.* **1952**, *56*, 195.
(35) Lawrance, G. A.; Stranks, D. A. *Inorg. Chem.* **1978,** *17*, 1804.

concentrated HCl, and 2.47 g of activated iron (44 mmol). The solution was refluxed for 12 h under a nitrogen atmosphere. The remaining iron was filtered, the ethanol evaporated under reduced pressure, and a solution of 20.6 g of Na_2H_2EDTA (55.3 mmol) in 60 mL of water added. The pH was raised to 9 with concentrated NH_4OH while the aqueous layer was extracted with 500 mL of CH_2Cl_2. The aqueous layer was washed with 100 mL of CH_2Cl_2, and the combined organic layers were dried over Na_2SO_4, filtered, and evaporated to dryness. The solid was dissolved in 50 mL of CH_2Cl_2/MeOH (95/5) and filtered over a thin layer of Alox. The Alox was washed with 200 of mL CH_2Cl_2/MeOH (95/5). The combined solutions were evaporated to dryness, and the solid was recrystallized in a mixture of CH_2Cl_2/hexane to give white crystals of **2**, melting at 129−131 °C. Yield: 425 mg (86%). ^{1}H-NMR in $CDCl_3$: δ 2.39 (s, 3H); 4.24 (s, 3H); 7.20−7.36 (m, 2H); 7.41 (dd, 1H, ^3J = 6.1 Hz); 7.63 (dd, 1H, ^3J = 7.9 Hz); 7.79 (dd, 1H, ^3J = 6.9 Hz); 8.25 (d, 1H, ^3J = 8.0 Hz); 8.50 (s, 1H). ^{13}C-NMR in $CDCl_3$: δ 18.52, 32.67 (primary C); 109.86, 119.93, 122.52, 123.15, 124.33, 137.41, 149.05 (tertiary C); 133.65, 137.39, 142.61, 148.04, 150.63 (quaternary C). EI-MS: *m/z* 223 ($M^{\bullet+}$). Anal. Calcd for $C_{14}H_{13}N_3$: C, 75.29; N, 18.82; H, 5.88. Found : C, 74.43; N, 18.53; H, 5.64.

Preparation of Complexes. Caution. Perchlorate salts with organic solvents are potentially explosive and should be handled with care.[36]

Preparation of $[Co_2(1b)_3](ClO_4)_4\cdot 4H_2O\cdot$MeOH. A 200 mg sample of ligand **1b** (0.41 mmol) was dissolved in 20 mL of CH_2Cl_2 and a solution of 106 mg (0.28 mmol) of $Co(ClO_4)_2\cdot 6H_2O$ in 20 mL of CH_3CN added. The solution, which turns orange instantaneously, was evaporated to dryness and dried under vacuum for 1 h. The solid was dissolved in a minimum of acetonitrile and methanol slowly diffused on it. The complex was obtained as orange crystals which were filtered. Concentration of the mother liquor afforded a second crop. Yield: 211 mg (78%). Anal. Calcd for $Co_2C_{93}H_{90}N_{18}Cl_4O_{16}\cdot 4H_2O\cdot$MeOH: Co, 5.67; C, 54.29; H, 4.94, N, 12.12. Found: Co, 5.71; C, 54.56; H, 5.00; N, 12.19. ^{1}H-NMR in CD_3CN, all signals are broad: δ −41.9 (s, 6H), −3.86 (s, 6H), 0.52 (s, 18H), 1.87 (s, 6H), 8.64 (s, 18H), 11.94 (s, 6H), 14.67 (s, 6H), 19.61 (s, 6H), 33.2 (s, 6H), 60.6 (s, 6H), 80.8 (s, 6H). IR (cm^{-1}): 3078, 2979 ($\nu_{CH_{aro}}$); 1609, 1585, 1539 ($\nu_{C=C}$, $\nu_{C=N}$); 1485, 1465 (δ_{CH_3}, δ_{CH_2}); 1093, 623 (ν_{ClO_4}). ES/MS (CH_3CN): *m/z* = 394.4 $[Co_2(\mathbf{1b})_3]^{4+}$, 559.0 $[Co_2(\mathbf{1b})_3(ClO_4)]^{3+}$.

Preparation of $[Co_2(1a)_3](ClO_4)_6\cdot 6H_2O$. A 250 mg sample of $[Co_2(\mathbf{1a})_3](ClO_4)_4$ (0.127 mmol) was dissolved in 100 mL of CH_3CN, and 420 μL of 30% H_2O_2 in water (0.38 mmol) and 230 μL of 7% $HClO_4$ in water were added with 2 mg of $[Cp_2Fe](BF_4)$ as catalyst. The solution was heated to 40 °C for 4 h with addition of 2 mg of $[Cp_2Fe](BF_4)$ each hour. The solution was cooled to room temperature and concentrated, and a saturated solution of $LiClO_4$ in water added until the solid began to precipitate. The solution was cooled to 4 °C, and the red-orange solid was filtered and dissolved in a minimum of acetonitrile. Methanol was slowly diffused to give red crystals which were filtered and dried (10^{-2} Torr, 4 h. 60 °C). The mother liquor was concentrated to give a second crop. Yield: 243 mg (88%). Anal. Calcd for $Co_2C_{87}H_{78}N_{18}Cl_6O_{24}\cdot 6H_2O$: Co, 5.36; C, 47.53; H, 4.13, N, 11.47. Found: Co, 5.57; C, 47.41; H, 3.96; N, 11.48. ES/MS: *m/z* = 946 $[Co_2(\mathbf{1a})_3(ClO_4)_4]^{2+}$; 597.2 $[Co_2(\mathbf{1a})_3(ClO_4)_3]^{3+}$; 423.0 $[Co_2(\mathbf{1a})_3(ClO_4)_2]^{4+}$; 318.6 $[Co_2(\mathbf{1a})_3(ClO_4)]^{5+}$; 249.0 $[Co_2(\mathbf{1a})_3]^{6+}$. ^{1}H-NMR in CD_3CN: δ 2.16 (s, 18H), 3.71 (s, 6H), 4.29 (s, 6H), 4.52 (s, 18H), 7.03 (s, 6H), 7.20 (s, 6H), 7.81 (d, 6H), 8.23 (d, 6H), 8.55 (d, 6H). ^{13}C-NMR in CD_3CN: δ 15.6, 19.5 (primary C); 43.2 (secondary C); 113.8, 115.0, 127.7, 129.7, 144.8, 154.1 (tertiary C); 135.7, 139.4, 141.0, 143.7, 150.9, 152.2 (quaternary C). IR (cm^{-1}): 3040, 3127 ($\nu_{CH_{aro}}$), 1612, 1586, 1546 ($\nu_{C=C}$, $\nu_{C=N}$), 1485, 1417 (δ_{CH_3}, δ_{CH_2}), 1090, 622 (ν_{ClO_4}).

Preparation of $(-)_{589}$-$[Co_2(1a)_3](ClO_4)_6$. A 47 mg sample of $[Co_2(\mathbf{1a})_3](ClO_4)_6\cdot 6H_2O$ was dissolved in 10 mL of acetonitrile. A 5 mL portion of water was added followed by addition of 5 mL of a saturated solution of $Na_2[(+)_{589}$-$(Sb_2(C_4O_6H_2)_2)]\cdot 5H_2O$[21] in water. The solution was concentrated until the beginning of crystallization. A 2 mL sample of acetonitrile was added and the solution heated to 80 °C to dissolve the solid. The solution was filtered hot and slowly cooled to room temperature. Fine red needles formed and were filtered. The mother liquor was then concentrated to give a second crop of crystals. The first crop was dissolved in 1 mL of acetonitrile and 10 mL of water, and the anions were exchanged with ClO_4^- loaded on a Dowex X3 anion exchange column. The solution was concentrated and the complex slowly recrystallized. The solid was filtered and dried under vacuum to give a $(-)_{589}$-$[Co_2(\mathbf{1a})_3](ClO_4)_6$ as a red solid. Yield: 10.0 mg (21%). $[\alpha]_{589} = -1022(4)°$, $[\alpha]_{578} = -1085(4)°$, $[\alpha]_{546} = -1681(5)°$ (T = 25 °C, acetonitrile). The second crop of crystals gives 18.9 mg of complex (54%) which is a nonracemic mixture of Δ and Λ isomers. Other analyses (^{1}H-NMR and IR) correspond to the racemic complex.

Preparation of $[Co_2(1b)_3](ClO_4)_6\cdot 8H_2O$. A 40 mg sample of $[Co_2(\mathbf{1b})_3](ClO_4)_4\cdot 4H_2O\cdot$MeOH (19.8 μmol) was dissolved in 5 mL of acetonitrile. A 5 mL portion of bromine was added and the solution refluxed for 12 h. The excess bromine was evaporated under reduced pressure and 10 mL of diethyl ether added to the solution. A red-orange precipitate formed which was filtered and suspended in 20 mL of acetonitrile containing 300 mL of $LiClO_4$. The mixture was refluxed for 1 h, filtered hot, and slowly cooled to room temperature. The solid obtained was filtered and dried under vacuum to give $[Co_2(\mathbf{1b})_3](ClO_4)_6\cdot 8H_2O$ as a red-orange solid. Yield: 29.6 mg (65%). Anal. Calcd for $Co_2C_{93}H_{90}N_{18}Cl_6O_{24}\cdot 8H_2O$: C, 48.18; H, 4.61; N, 10.87. Found: C, 48.05; H, 4.42; N, 10.69. ^{1}H-NMR in CD_3CN: δ 1.71 (t, 18H, ^3J = 7.4 Hz, br), 2.30 (s, 18H), 3.62 (s, 6H, br), 4.42 (s, 6H), 4.95 (q, 12H, ^3J = 7.4 Hz, br), 7.02 (s, 6H, br), 7.20 (d, 6H, br), 7.84 (d, 6H), 8.22 (d, 6H, br), 8.40 (d, 6H). ^{13}C-NMR in CD_3CN: δ 15.5, 19.5 (primary C); 41.4, 43.1 (secondary C); 113.9, 115.0, 127.7, 129.8, 144.9, 154.0 (tertiary C); 135.7, 139.4, 141.0, 143.8, 144.5, 150.9 (quaternary C). IR (cm^{-1}): 3120, 3080, 2983, 2940 ($\nu_{CH_{aro}}$); 1612, 1586 ($\nu_{C=C}$, $\nu_{C=N}$); 1465, 1383 (δ_{CH_3}, δ_{CH_2}); 1088, 622 (ν_{ClO_4}); 789, 718, 692 ($\delta_{CHaro.}$). ES/MS (CH_3CN): *m/z* = 262.8 $[Co_2(\mathbf{1b})_3]^{6+}$, 335.4 $[Co_2(\mathbf{1b})_3(ClO_4)]^{5+}$, 444.0 $[Co_2(\mathbf{1b})_3(ClO_4)_2]^{4+}$, 625.4 $[Co_2(\mathbf{1b})_3(ClO_4)_3]^{3+}$, 987.6 $[Co_2(\mathbf{1b})_3(ClO_4)_4]^{2+}$.

Preparation of $[Co(2)_3](ClO_4)_2\cdot$MeOH. A 223 mg sample of **2** (1 mmol) was dissolved in 5 mL of CH_2Cl_2/CH_3CN (1/1) and 5 mL of CH_3CN containing 122 mg (0.33 mmol) of $Co(ClO_4)_2\cdot 6H_2O$ added. The orange solution was stirred for 5 min and evaporated to dryness. The solid was dissolved in 2.5 mL of acetonitrile and methanol slowly diffused to give, after filtration, orange crystals of $[Co(\mathbf{2})_3](ClO_4)_2\cdot$MeOH. Yield: 306 mg (96%). Anal. Calcd for $CoC_{42}H_{39}N_9Cl_2O_8\cdot CH_3OH$: C, 53.80; N, 4.52; H, 13.13. Found: C, 53.39, N, 4.42; H, 13.27. ^{1}H-NMR in CD_3CN (22 °C, all signals singlets): *fac* isomer, δ −0.2, 3.6, 12.6, 35.0, 79.9 (single protons), 1.6, 17.2 (methyl protons); *mer* isomer, δ −4.1, −2.6, 0.3, 5.0, 7.5, 10.8, 13.4, 14.2, 17.7, 34.9, 47.8, 49.1, 51.8, 64.2, 91.2 (single protons), −8.8, −6.8, 4.5, 14.9, 28.6. 30.3 (methyl protons); eight protons appeared as very broad signals and could not be attributed to *mer* or *fac* isomers, δ −50.2, −26, −21.0, 5.9, 21.0, 48.0, 73.2, 107.8.

Spectroscopic and Analytical Measurements. UV−vis spectra were recorded at 22 °C in acetonitrile or dichloromethane on a Perkin-Elmer Lambda 5 spectrophotometer with quartz cells of 1 and 0.1 cm path length. The spectrophotometric titrations were recorded on a computer driven Perkin-Elmer Lambda 5 as previously described.[13] Infrared spectra were recorded on a Perkin-Elmer IR 883 as KBr pellets with wavenumbers in inverse centimeters. EI-MS spectra (70 eV) were recorded with VG 7070E and Finnigan 4000 spectrometers. Elemental analyses were performed by Dr. H. Eder of the Microchemical Laboratory of the University of Geneva. Metal contents were determined by atomic absorption (Pye Unicam SP9) after acidic oxidative mineralization of the complexes.

ES-MS spectra were recorded on a Finnigan-Mat SSQ 7000 spectrometer at the Mass Spectrometry Laboratory of the University of Geneva. For a typical kinetic experiment followed by ES-MS, equal volumes of each solution of complexes or of ligands, of about 10^{-5} M concentration, were mixed at time zero. Spectra were then recorded at regular intervals, taking as time t the time of detection of the species. Relative intensities of the peaks corresponding to $[Co_2(\mathbf{1a})_{3-x}(\mathbf{1b})_x]^{4+}$ (x = 0−3) were measured and weighted by the sum of the total intensity of these signals to give the relative percentages of each detected species.

CD spectra were recorded on a Jasco 710 spectrometer using thermostated quartz cells of 0.5, 1, and 2 cm path length. The resolution

(36) Wolsey, W. C. *J. Chem. Educ.* **1978**, *55*, A355.

was 1 nm, the sensitivity 0.020°, and the time response 1s. For a typical kinetic experiment followed by CD, spectra were recorded at regular intervals for a total of at least 4 half-lifes. $\Delta\theta$ values as a function of time are collected for 10 wavelengths showing maximum variations in the intensity of the signal. These wavelengths were collected in an interval of 50 nm. The evolution of $\Delta\theta$ as a function of t for each wavelength was fitted to a decreasing exponential model with a nonlinear least squares algorithm. The fitting gives the rate of decrease at the 10 wavelengths, and the average value affords the racemization rate of the complex and its standard deviation.

^{1}H-NMR spectra and ^{13}C-NMR spectra for characterization at room temperature and pressure were recorded on a Varian Gemini 300 with tetramethylsilane (TMS) as the inner reference. Chemical shifts are given in parts per million, and abbreviations are as follows: s, singlet; d, doublet; t, triplet; q, quadruplet; m, multiplet; br, broad. Variable temperature and pressure ^{1}H-NMR spectra were recorded on a Bruker ARX 400 spectrometer, with solutions 10^{-2} M in $[Co(\mathbf{2})_3]^{2+}$ in acetonitrile and with TMS as the shift and line width reference. The ambient pressure measurements were followed in a commercial thermostated probe, and the temperature was found to be constant within $\pm$0.2 K as measured by a substitution technique.[37] Variable pressure measurements were made up to 200 MPa using a high-pressure probe.[38] The variable temperature (variable pressure) ^{1}H-NMR spectra were obtained using a 90° pulse length of 6 μs (17 μs) in the quadrature detection mode, with 64K data points resulting from 64 (256) scans accumulated over a total spectral width of 45 450 Hz. Transversal relaxation times, T_2, were obtained by deconvolution of peaks into Lorentzian curves using the program Anaspec[39] (Bruker ARX 400). T_2 values were then corrected for field inhomogeneity and line broadening by subtraction of the width at half-height of the TMS signal. The analysis of the experimental data was accomplished by a nonlinear least squares program fitting the values of the desired parameters.[40] Reported errors are 1 standard deviation.

Acknowledgment. We thank Mr. Werner Kloeti for running the ESMS spectra and Dr. Markus Albrecht (University of Karlsruhe) for supplying coordinates of an X-ray structure. This research was supported by the Swiss National Science Foundation.

Supporting Information Available: Relaxation of the ^{1}H NMR signal as a function of temperature and pressure (Tables S1 and S2) (2 pages). See any current masthead page for ordering and Internet accesss instructions.

JA963693L

(37) Amman, C.; Meier, P.; Merbach, A. E. *J. Magn. Reson.* **1982**, *46*, 319.

(38) Merbach, A. E.; Frey, U.; Helm, L.; Roulet, R. In *Advanced Applications of NMR to Organometallic Chemistry*; Gielen, M., Willem, R., Wrackmeyer, B., Eds.; John Wiley & Sons: Chichester, 1996; p 199.

(39) Helm, L. Program Library, University of Lausanne, 1996.

(40) Program Scientist, Version 2.0, MicroMath Inc., 1995.